ASSESSMENT AND COMPARISON OF LARGE EDDY SIMULATIONS IN ASYMMETRICALLY HEATED AND HIGHLY TURBULENT CHANNEL FLOWS

Martin David, Adrien Toutant, Françoise Bataille

ASSESSMENT AND COMPARISON OF LARGE EDDY SIMULATIONS IN ASYMMETRICALLY HEATED AND HIGHLY TURBULENT CHANNEL FLOWS

M. David[⋆]*, A. Toutant*[⋆] *and F. Bataille*[⋆]

[⋆] *PROMES-CNRS (UPR 8521), Université de Perpignan via Domitia Technosud - Rambla de la thermodynamique, 66100 Perpignan – France*
martin.david@promes.cnrs.fr

Abstract

This study concerns turbulent flow submitted to high heat transfer and characterized by a strong coupling between temperature and turbulence. This kind of configuration is encountered in gas-pressurized receivers of concentrated solar power tower plants. To improve knowledge of turbulence in the case of large temperature gradient and its modeling, both Direct Numerical Simulation (DNS) and Large Eddy Simulations (LES) of the anisothermal flow in asymmetrically heated channels are performed. Two different types of heating, representing the middle and the end of the solar receiver, are studied. Two types of heating are investigated. In the first case, the mean fluid temperature is below the cold wall temperature, meaning that it is heated from the both walls. In the second case, the mean fluid temperature is between the two wall temperatures. These two configurations induce opposite directions of the velocity in the wall-normal direction near the cold wall. Several LES models coupled with thermal models are used and compared with data provided by DNS carried out in both types of heating. The results highlight the good results of the tensorial formulation of the Anisotropic-Minimum-Dissipation model.

1 Introduction

Concentrated Solar Power (CSP) systems are capable of storing energy by use of thermal energy storage technologies and are then very attractive for large-scale power generation. Solar power tower functioning with gas-pressurized solar receivers allow to reach very high fluid temperature and produce a high-quality energy. Moreover, to produce electricity, the solar receivers are included in a Brayton cycle that permits reaching are heat-to-power conversion efficiency. In these devices, the heat transfer to the fluid is critical since it directly impacts the efficiency of the cycle. As the heat transfer is strongly influenced by the flow parameters (David *et al.* 2021), accurate and accessible tools are required to study the solar receiver.

Large Eddy Simulations (LES) model the small scales in order to reproduce their effect of the larger ones, which are resolved. This Computational Fluid Dynamic (CFD) approach provides more accurate and detailed results than the ones of Reynolds Averaged Navier-Stokes (RANS) simulations. Their computational cost is also much more reasonable than the one of Direct Numerical Simulation (DNS). Hence, LES offers an interesting compromise. With the increase in computer performance, LES should become widely used in the industry. For that reason, the investigation of LES models in various conditions is valuable. *A posteriori* tests of Large Eddy Simulation are commonly performed in the literature (Stolz *et al.* 2001, Horiuti 1989, Dupuy *et al.* 2019). LES at high Reynolds numbers are more recently studied (Kremer and Bogey 2015, Streher *et al.* 2021). The investigations of anisothermal flows are quite unusual despite their importance in the industry. Among those studies, very few take into account the coupling between the temperature and the dynamic (Serra *et al.* 2012, Dupuy *et al.* 2019, David *et al.* 2021).

To the author's knowledge, there is no study of LES in anisothermal channel flow heating from both sides in the literature. Nevertheless, this configuration is widely encountered in many engineering systems, such as heat exchangers or the gas-pressurized solar receivers. The present paper aims to fulfill this gap. Its outline is the following. In Section 1, the study configuration is detailed. Then, the results are given and discussed in Section 2. Lastly, a final section concludes.

2 Study configuration

Flow modeling

The Navier-Stokes equations are solved under the low Mach number proposed by Paolucci (Paolucci 1982). The ideal gas law is used to close the system. The thermal dilatation and the fluid property variations are taken into account. The Sutherland's law (Sutherland 1893) is used to computed the dynamic viscosity. To study various temperature profiles, *i.e.* various axial location in the solar receiver, a heat source, H_s, is introduced in the energy equation. The two most significant subgrid terms highlighted by Dupuy *et al.* (Dupuy *et al.* 2019) are considered: a

subgrid term related to the velocity-velocity correlation and another modeling the density-velocity correlation. Functional and structural models are studied. The Anisotropic-Minimum-Dissipation (AMD) model proposed by Rozema *et al.* (Rozema *et al.* 2015) and the $H^{(4)}$ tensorial model version of the AMD model proposed by Dupuy (Dupuy *et al.* 2019) are investigated. As for the structural approach, the scale-similarity model proposed by Bardina *et al.* (Bardina *et al.* 1980) is assessed. The same model is used to compute both the subgrid-scale stress tensor and the subgrid-scale heat flux. The tensorial AMD model is associated with the scalar AMD (Abkar *et al.* 2016) model for the modeling of the subgrid-scale heat flux.

Numerical settings

The new generation of solar power towers functioning with gas-pressurized solar receivers allows to reach very high fluid temperature and, thus, to enhance the efficiency of the heat-to-power conversion. These absorbers are characterized by very complex flows. Indeed, they involve highly turbulent flows in order to enhance the wall heat flux and facilitate fluid heating. The solar receivers are a built-in cavity to lower the heat losses. For that reason, only one wall of the solar receiver is irradiated. This induces asymmetric heating of the fluid. To reproduce these conditions, large-eddy simulations are carried out in a fully developed three-dimensional turbulent channel flow asymmetrically heated, see Figure 1. The streamwise (x)

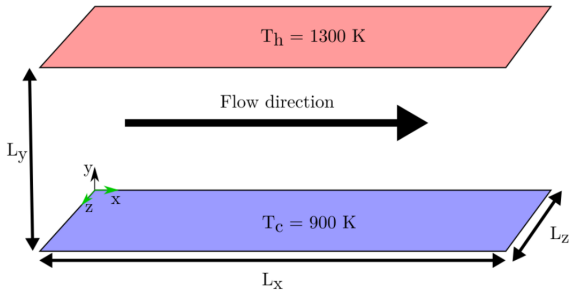

Figure 1: Channel flow geometry.

and spanwise (z) directions are periodic. The flow is bounded by two plane walls in the wall-normal direction (y). The domain size is $4\pi\delta \times 2\delta \times 4/3\pi\delta$ with $\delta = 3$mm. The volume of the studied channel is 2.8×10^{-6} m^3. The meshes of the anisothermal DNS and LES are respectively composed of 660 million and 2.3 million cells. The points are distributed as follow: $N_x^{DNS} \times N_y^{DNS} \times N_z^{DNS} = 1152 \times 746 \times 768$ for the DNS, and $N_x^{LES} \times N_y^{LES} \times N_z^{LES} = 160 \times 152 \times 96$ for the LES. The streamwise and spanwise directions are discretized with constant cell size. In the wall-normal direction, the mesh follows a hyperbolic tangent law. The temperatures of the walls are 1300 K for the hot wall and 900 K for the cold wall. A streamwise volume force is added to the channel to maintain a constant mass flow rate. TrioCFD software (Calvin *et al.* 2002) is used to perform simulations. Calculations are carried out operating a finite difference method in a staggered grid system.

Table 1: Friction Reynolds numbers.

Name	Re_τ^c	Re_τ^h	Re_τ^{mean}
LT simulations	1000	640	820
HT simulations	970	630	800

Table 2: Grid spacing of the DNS and LES meshes. The dimensionless cell sizes are computed at the cold wall (highest friction Reynolds number).

Name	Dimensionless cell size Δ_x^+ ; $\Delta_y^+(0)$; $\Delta_y^+(\delta)$; Δ_z^+
DNS (LT)	10.9 ; 0.42 ; 5.4 ; 5.4
DNS (HT)	10.7 ; 0.41 ; 5.3 ; 5.3
LES (LT)	78 ; 1.1 ; 32 ; 43
LES (HT)	77 ; 1.0 ; 32 ; 43

Investigated cases

Two different types of heating, representing the middle and the end of the solar receiver, are studied. They are performed at the same wall friction. In the first case, the mean fluid temperature is below the cold wall temperature, meaning that it is heated from the both walls. In the second case, the mean fluid temperature is between the two wall temperatures. These two configurations induce opposite directions of the velocity in the wall-normal direction near the cold wall. For practical reasons, the associated simulations are respectively denoted as low fluid temperature (LT) and high fluid temperature (HT). They respectively correspond to heat sources of $H_s = -54635$ kW/m^3 and $H_s = 0$. In the first case, the negative heat source removes heat from the flow which leads to the lowering of the fluid temperature. The Reynolds numbers, based on the hydraulic diameter and the bulk velocity, are 82 000 for the LT simulations and 60 000 for the HT simulations. The obtained friction Reynolds numbers are listed in Table 1. The bulk temperatures are respectively 1093 K and 883 K. The main characteristics of the meshes are given in Table 2.

3 Results and discussion

Functional models are traceless meaning that only the deviatoric Reynolds stresses can be reconstructed and compared to DNS data without filtering process:

$$\langle u_i' u_j' \rangle^{dev} = \langle u_i' u_j' \rangle - \frac{1}{3} \langle u_k' u_k' \rangle \delta_{ij}, \qquad (1)$$

where δ_{ij} is the Kronecker symbol. To facilitate the comparison between LES and DNS, the modeled terms are systematically added to the associated quan-

tity.

$$\langle u_i' u_j' \rangle^{DNS,dev} = \langle u_i' u_j' \rangle^{LES,dev} + \langle \tau_{ij}^{SGS}(\mathbf{U}, \overline{\Delta}) \rangle^{dev}, \quad (2)$$

with $\langle u_i' u_j' \rangle = \langle U_i U_j \rangle - \langle U_i \rangle \langle U_j \rangle$ and $\langle u_i' u_j' \rangle^{LES} = \langle \widetilde{U}_i \widetilde{U}_j \rangle - \langle \widetilde{U}_i \rangle \langle \widetilde{U}_j \rangle$. τ_{ij} is the subgrid-scale tensor associated with the Reynolds stresses. The coordinates x_1, x_2, x_3 and x, y, z as well as U_1, U_2, U_3 and U, V, W are used interchangeably for simplicity. The same procedure is applied to the correlations of velocity and temperature:

$$\langle u_i' \theta' \rangle^{DNS} = \langle u_i' \theta' \rangle^{LES} + \langle \pi_i^{SGS}(\mathbf{U}, T, \overline{\Delta}) \rangle, \quad (3)$$

with $\langle u_i' \theta' \rangle^{DNS} = \langle U_i T \rangle - \langle U_i \rangle \langle T \rangle$ and $\langle u_i' \theta' \rangle^{LES} = \langle \widetilde{U}_i \widetilde{T} \rangle - \langle \widetilde{U}_i \rangle \langle \widetilde{T} \rangle$. π_i is the density-velocity subgrid term.

In this section, the LES are assessed on the DNS performed in both heating conditions. The results are normalized thanks to the classical scaling "+". It involves the friction velocity and the friction temperature, respectively defined as $U_\tau = \sqrt{\nu \partial U / \partial y}$, and $\theta_\tau = \phi_w / (\rho C_p U_\tau)$, where ν is the kinematic viscosity, C_p is the heat capacity at constant pressure, and ϕ_w is the conductive heat flux at the wall. The LES and DNS results are temporally averaged and spatially averaged along with the homogeneous directions. This combination of averages is denoted by $\langle \cdot \rangle$. The wall-normal profiles are displayed in the next. The first-order statistics are firstly exposed then the second-order statistics are investigated. In addition to the LES performed with turbulence models, a LES without a model is investigated and denoted "ILES".

First-order statistics

First-order statistics give the global behavior of the flow. Figure 2 exposes the wall-normal profiles of streamwise, wall-normal, and temperature. The results show that the streamwise velocity is mitigated in the simulation with low fluid temperature. The wall-normal velocity profile is substantially affected by the temperature distribution. Indeed, while it is negative and with the same magnitude in the case without source term, the wall-normal velocity is asymmetric in the low-temperature case. On the hot side, the magnitude is almost three time higher in the simulation with heat source. On the cold side, the wall-normal velocity is opposed between the two studied heating conditions. The dimensionless temperature profiles on the cold side traduce the difference between the two investigated cases. Regarding the LES results, the tendency of each profile is respected. The AMD model tends to overestimate the streamwise velocity profile while the other LES are relatively accurate. The wall-normal velocity is better predicted by the LES with functional models. The temperature profiles are quite well approximated by the tensorial AMD model. Overall, the quality of the estimation provided by each model is weakly dependent on the heating conditions.

Second-order statistics

The second-order statistics permit investigating the flow in detail. The velocity correlations give information on the turbulent scales. They are exposed in Figure 3. The correlations of streamwise, spanwise, and wall-normal velocities are quite similar: they follow a bell shape and reach a maximum of magnitude around $y^+ = 13$. The DNS carried out with a source term, "DNS [LT]" exhibits lower velocity fluctuations than the simulation "DNS [HT]" and the peak is reached slightly closer to the walls. The extrema of the $\langle u'v' \rangle^+$ correlation are also mitigated when compared to the DNS without source term. The LES tend to overestimate the streamwise, spanwise, and wall-normal velocity correlations. The scale-similarity model seems to be not enough dissipative which explains its significant overestimation of the peaks. The tensorial AMD model produces the best results on these values. The tensorial formulation permits improving the results of the AMD model and is able to capture the anisotropy of the flow. The cross-velocity correlation is well approximated by all the LES models.

The correlations involving the temperature are given in Figure 4. The DNS results show that the magnitude of the correlation of streamwise velocity and temperature is mitigated in the case of the DNS with source term. The peaks are slightly shifted toward the walls. On the cold side, a secondary peak is observed close to the center of the channel. It is due to the temperature distribution. The correlation of wall-normal velocity and temperature is significantly influenced by the heat source. In the simulation with a lower bulk temperature than the cold wall temperature, the profile becomes positive on the cold side after $y^+ = 450$. On the hot side, it reaches a minimum at $y^+ = 50$. The temperature fluctuations are given on the bottom graph. They exhibit a peak around $y^+ = 13$, as for the velocity correlations. Once again, in the "DNS [LT]", the peak is reached slightly closer to the wall. In the simulation "DNS [HT]" a third peak is observed in the center of the channel while in the simulation with a heat source, it does not exist due to the highly asymmetric temperature fluctuations. The minimum is obtained for $y^+ = 300$. The AMD model and the tensorial AMD model produce satisfying results on the correlation of streamwise velocity and temperature. All the models produce quite good estimations of the correlation of wall-normal and temperature, the tensorial AMD model provides the most accurate estimation on both sides. The temperature fluctuations are poorly approximated by the LES. The AMD model is the closest to the DNS results.

The comparison of the LES performance on the second-order statistics shows that, as for the first-order statistics, the quality of the approximation provided by each model is weakly dependent on the heating conditions.

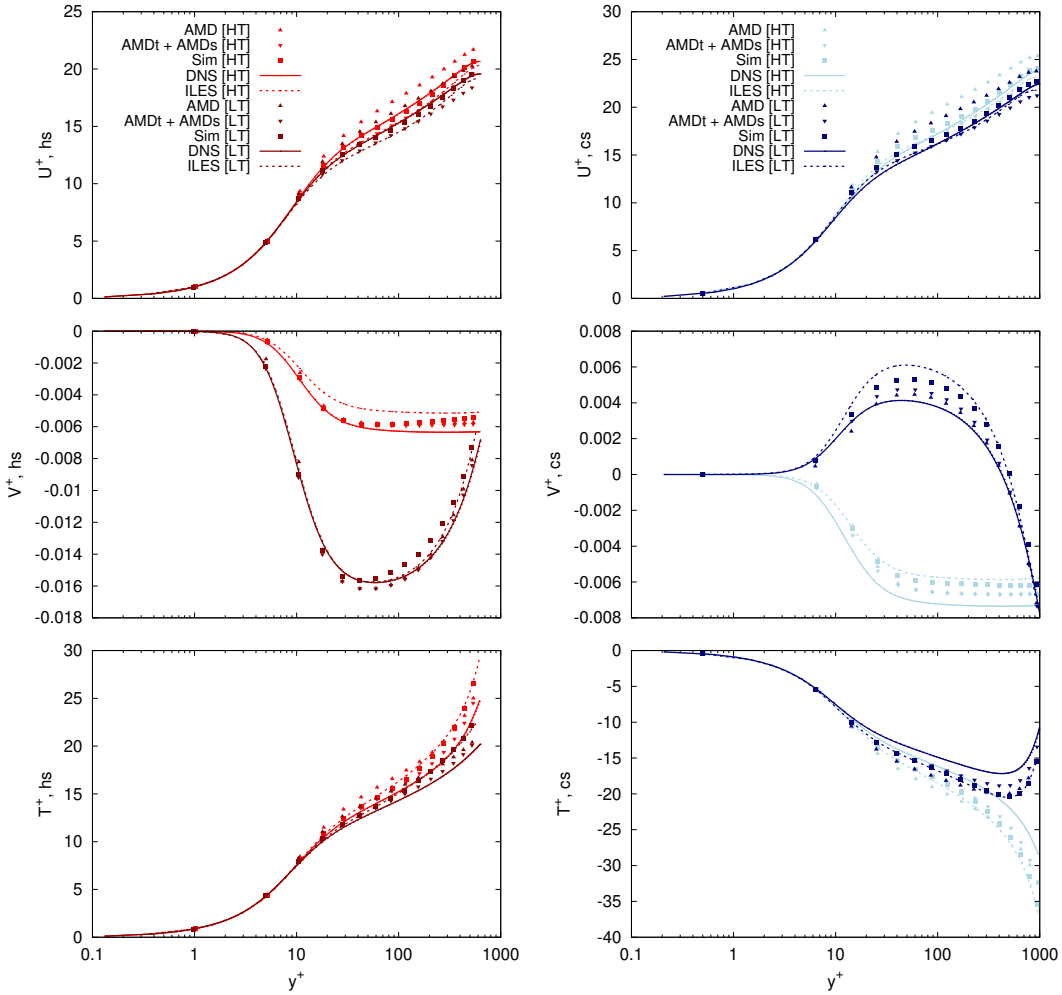

Figure 2: Wall-normal profiles of mean quantities. The hot, respectively cold, profiles are plotted on the left, respectively right.

4 Conclusions

Direct Numerical simulations and Large Eddy simulations have been performed in asymmetrically heated turbulent channel flows in the operating conditions of solar receivers. Two different types of heating, representing the middle and the end of the solar receiver, have been studied thanks to the introduction of a heat source in the energy equation. In the first case, the mean fluid temperature is below the cold wall temperature, meaning that it is heated from the both walls. In the second case, the mean fluid temperature is between the two wall temperatures. Functional and structural models of LES have been studied in the two different heating conditions.

The results show that the physic of the flow is significantly impacted by the temperature profiles. The wall-normal velocity has opposite directions near the cold wall depending on the heating case. The fluctuations tend to be mitigated in the case of a mean fluid temperature below the cold wall temperature.

Regarding the performance of the LES, it seems that the scale-similarity model is not enough dissipative. The AMD and the tensorial version of the AMD model produce satisfying results. The tensorial AMD model is particularly valuable to estimate the velocity correlations due to its ability to capture the anisotropy of the flow.

Acknowledgments

This work was granted access to the HPC resources of CINES under the allocation 2020-A0082A05099 made by GENCI. The authors acknowledge PRACE for awarding them access to Joliot-Curie at GENCI@CEA, France (PRACE Project : 2020225398). The authors gratefully acknowledge the CEA for the development of the TRUST platform. The authors gratefully acknowledge the Occitania region for their funding of the thesis grant.

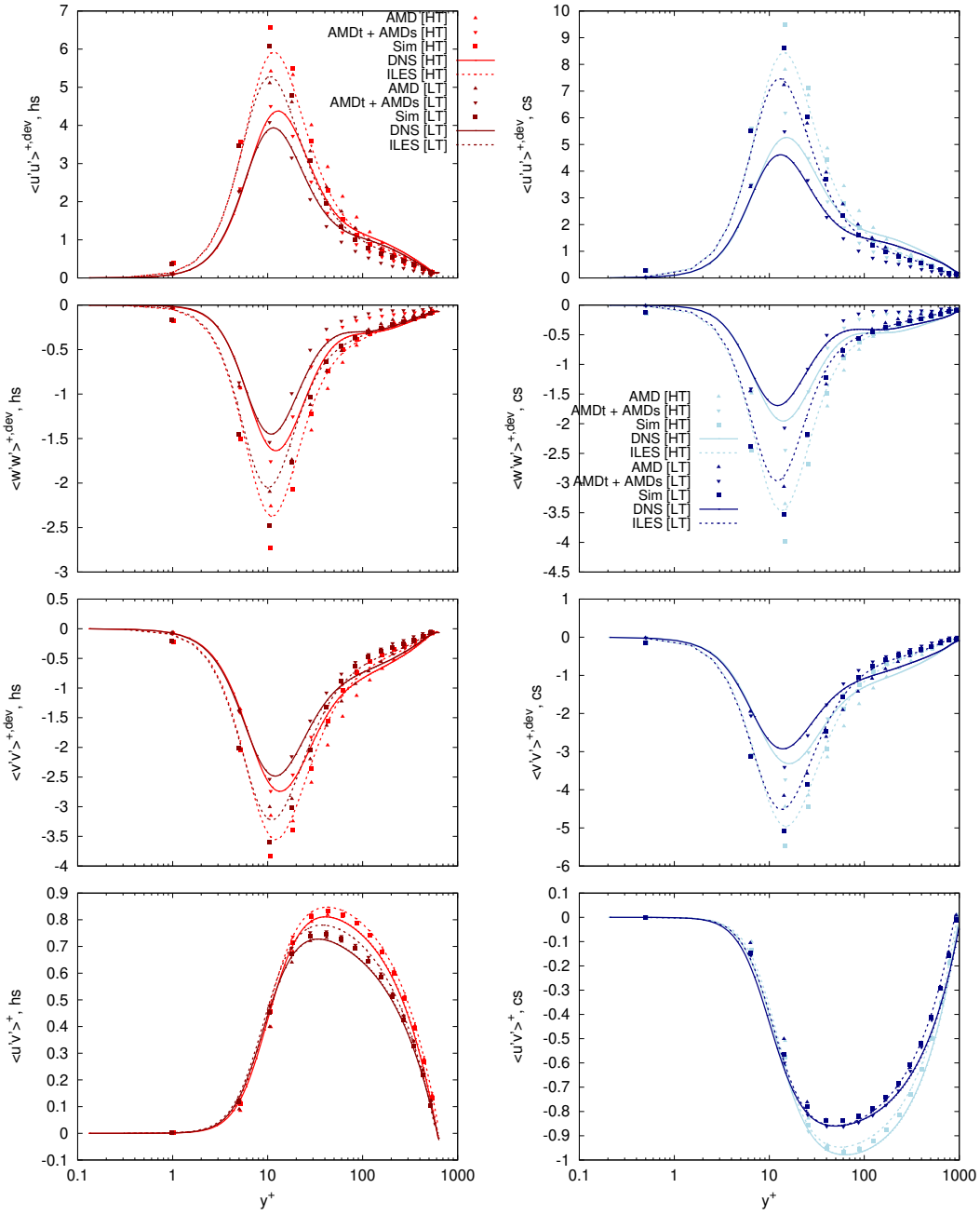

Figure 3: Wall-normal profiles of velocity correlations. The hot, respectively cold, profiles are plotted on the left, respectively right.

References

Abkar, M., Bae, H. J., and Moin, P. (2016). Minimum-dissipation scalar transport model for large-eddy simulation of turbulent flows. *Physical Review Fluids*, 1(4):041701.

Bardina, J., Ferziger, J., and Reynolds, W. (1980). Improved subgrid-scale models for large-eddy simulation. In *13th Fluid and PlasmaDynamics Conference*, Fluid Dynamics and Co-Located Conferences. American Institute of Aeronautics and Astronautics.

Calvin, C., Cueto, O., and Emonot, P. (2002). An object-oriented approach to the design of fluid mechanics software. *ESAIM: Mathematical Modelling and Numerical Analysis - Modélisation Mathématique et Analyse Numérique*, 36(5):907–921.

David, M., Toutant, A., and Bataille, F. (2021). Numerical development of heat transfer correlation in asymmetrically

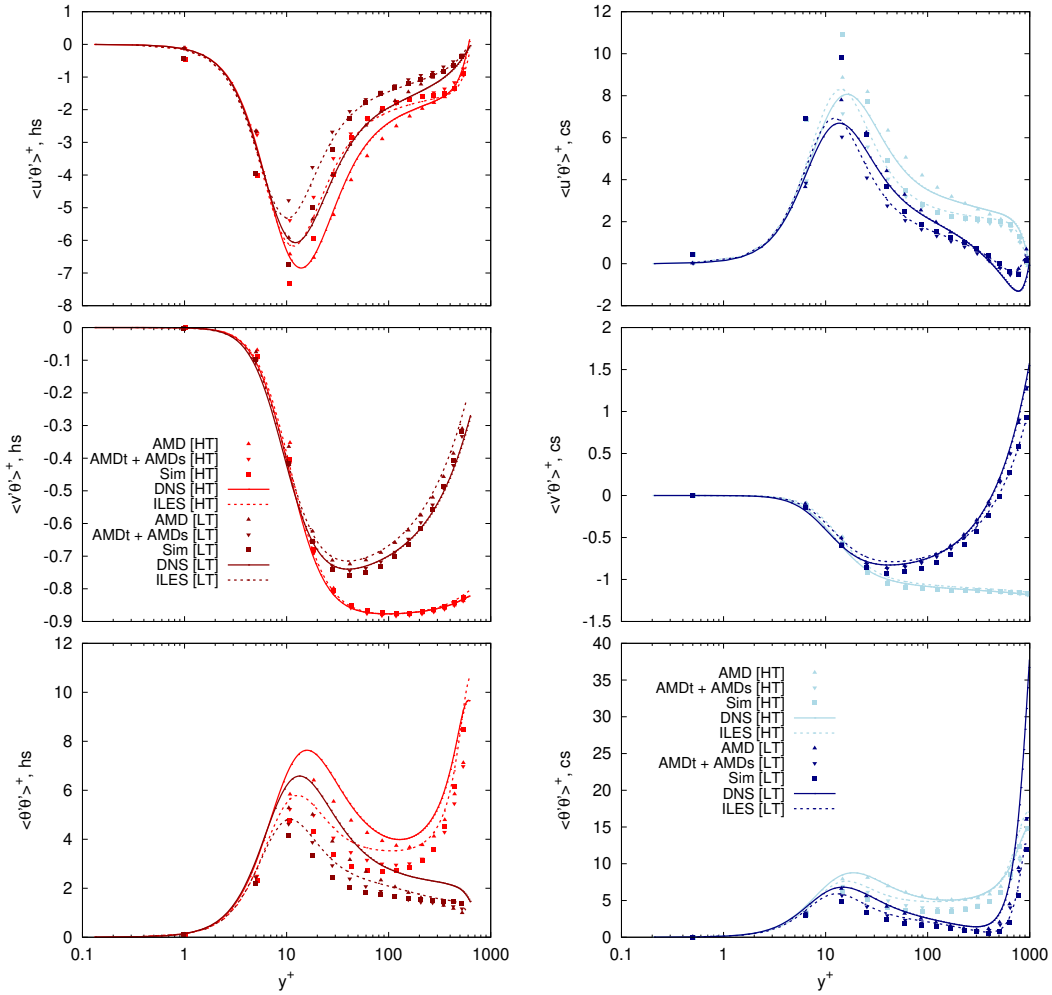

Figure 4: Wall-normal profiles of correlations involving temperature. The hot, respectively cold, profiles are plotted on the left, respectively right.

heated turbulent channel flow. *International Journal of Heat and Mass Transfer*, 164:120599.

Dupuy, D., Toutant, A., and Bataille, F. (2019). A posteriori tests of subgrid-scale models in an isothermal turbulent channel flow. *Physics of Fluids*, 31(4):045105.

Dupuy, D., Toutant, A., and Bataille, F. (2019). A posteriori tests of subgrid-scale models in strongly anisothermal turbulent flows. *Physics of Fluids*, 31(6):065113.

Ho, C. K. and Iverson, B. D. (2014). Review of high-temperature central receiver designs for concentrating solar power. *Renewable and Sustainable Energy Reviews*, 29:835–846.

Horiuti, K. (1989). The role of the Bardina model in large eddy simulation of turbulent channel flow. *Physics of Fluids A: Fluid Dynamics*, 1(2):426–428.

Kremer, F. and Bogey, C. (2015). Large-eddy simulation of turbulent channel flow using relaxation filtering: Resolution requirement and Reynolds number effects. *Computers and Fluids*, 116:17–28.

Paolucci, S. (1982). Filtering of sound from the Navier-Stokes equations. *NASA STI/Recon Technical Report N*, 83.

Rozema, W., Bae, H. J., Moin, P., and Verstappen, R. (2015). Minimum-dissipation models for large-eddy simulation. *Physics of Fluids*, 27(8):085107.

Serra, S., Toutant, A., and Bataille, F. (2012) Thermal Large Eddy Simulation in a Very Simplified Geometry of a Solar Receiver. *Heat Transfer Engineering*, 33(6):505-524

Stolz, S., Adams, N. A., and Kleiser, L. (2001). An approximate deconvolution model for large-eddy simulation with application to incompressible wall-bounded flows. *Physics of Fluids*, 13(4):997–1015.

Streher, L. B., Silvis, M. H., Cifani, P., and Verstappen, R. W. C. P. (2021). Mixed modeling for large-eddy simulation: The single-layer and two-layer minimum-dissipation-Bardina models. *AIP Advances*, 11(1):015002.

Sutherland, W. (1893). The viscosity of gases and molecular force. *The London, Edinburgh, and Dublin Philosophical Magazine and Journal of Science*, 36(223):507–531.